Int. J. Heat Mass Transfer. Vol. 26, No. 2, pp. 185-196, 1983
Printed in Great Britain

0017-9310/83/020185-12 $03.00/0
Pergamon Press Ltd.

FREE ENERGY LOSS DURING THE BREAKDOWN OF LIQUID FILMS

D. J. RYLEY and XU TINGXIANG*
Department of Mechanical Engineering, University of Liverpool, Liverpool L69 3BX, U.K.

(*Received* 6 *April* 1982 *and in final form* 1 *July* 1982)

Abstract—This study arose as an annexe to an ongoing investigation of the breakdown behaviour of liquid films traversing the stator blades of operating wet steam turbines. The plane surface of a horizontal glass block is treated so that some areas are wetted by water and others are water-repellant. A circular area (wettable, 'drop') was surrounded by an annulus (non-wetting) in turn surrounded by a second narrow annulus (wettable, 'ring'), all circles being concentric. A liquid film is formed over the whole area within the outer circle. This is diminished in thickness until perforation occurs and the residual water collects on and covers each of the wettable areas. Measurements of height and of liquid mass are made both for the original film and later for the drop and the ring. These measurements permit the calculation both of the original free energy and aggregate final free energies. An energy loss occurs which can be related to the mass of the film and the geometry of the prepared surfaces and can be calculated by suitably modelling the profiles of the ring and drop by geometric shapes which permit analysis. A circular segment gave the best fit. Contact angles calculated from the modelled profiles were checked by measurements on photographic silhouettes. Two new dimensionless numbers were introduced into the analysis; $He = \rho g H_C^2/2\sigma_{LG}$ which is the ratio of the potential energy to the surface energy for a liquid component and $Ae = \rho g A_C/\sigma_{LG}$ which is related to the ratio of the diameter of the solid surface wetted by the original film to the film thickness.

NOMENCLATURE

A, area, LG interface area;
D, specific dimension of drop or ring;
E, energy;
F_1, F_2, F_3, functions;
G, centre of gravity;
g, gravitational constant;
H, height or thickness;
i, order of designation of liquid fragment;
M, mass;
n, number of liquid fragments;
Q, free energy loss;
R, radius of circle;
U, specific bound energy;
V, liquid volume.

Greek symbols

ρ, liquid density;
θ, contact angle;
σ, surface tension;
ξ, loss coefficient.

Dimensionless quantities

$\bar{H}$, height;
Ae, area;
He, energy ratio.

Subscripts

a, air, vapour or gas;
l, liquid;
1, initial, before film breakdown;
2, final, after film breakdown;
D, drop;
R, ring;
F, free;
P, liquid component parts after breakdown;
T, total;
C, liquid film;
Q, interface between liquid fragment and solid surface;
S, system;
g, to centre of gravity;
M, refers to inner diameter of ring;
E, refers to outer diameter of ring;
min, minimum;
cal, calculation;
mea, measurement;
LG, liquid-gas interface;
SG, solid-gas interface;
LS, liquid–solid interface.

* Permanent address: Department of Power Machinery Engineering, Xi'an Jiaotong University, Xi'an, China.

1. INTRODUCTION

IT IS well known that nucleated fog droplets, deposited by diffusion onto the stator blades of the post-condensation stages in wet steam turbines, collect into rivulets which are propelled by gravity and vapour shearing forces to the blade trailing edge. Drops of 'coarse water' are torn therefrom and these drops are responsible for erosion damage in the downstream rotor blade rings. The rivulets pursue a tortuous path across the stator blade surfaces and may change their paths with the passage of time as usage alters the local wetting characteristics of the surfaces. These changes may influence erosion.

The stability of films on steam turbine blades, nuclear reactor tube surfaces and in chemical engineering generally has been widely investigated. Among other workers Hartley and Murgatroyd [1] and Murgatroyd

[2] studied the break-up of isothermal flowing fluids and their stability under shear and form forces. Films draining down planes were studied by Bankoff [3] and by Mikielewicz and Moszyinski [4]. Films, rivulets and dry patches in steam swept flow on horizontal and inclined plates were studied by Khoshaim [5].

Students of film breakdown frequently appeal to the well-known criterion of minimum free energy. According to this criterion a liquid film which has less than the minimum stable thickness will perforate because if it remained as a film its free energy would exceed the value of the aggregate free energy contained in the fragments. Rupture of the film is a spontaneous event. It is irreversible; it incurs an entropy increase and involves the dissipation of energy as heat.

The present writers observed that the disposition of liquid fragments after film breakdown is influenced by the wettability of the surface; discrete masses of liquid tending to occupy those areas of the underlying surface which were most readily wetted. This observation suggested the basis for the work to be described in which an appeal would be made to the minimum free energy criterion. Because of the difficulty of controlling the breakdown of a moving film to provide a situation amenable to analysis by this criterion, we decided to make the first attempt using a stationary film. We hoped thus to discover patterns of behaviour which would be expected to occur also in the breakdown of a moving film.

Because of the energy loss during film breakdown there will be a finite difference between the aggregate free energy present in the intact film at the point of breakdown and that present after breakdown when the resulting components have regained stability. Provided sufficiently accurate measurements can be made it should be possible to find the magnitude of this loss. So far as we know this has not previously been attempted.

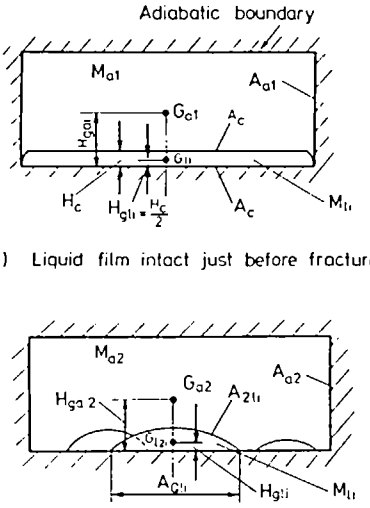

(a) Liquid film intact just before fracture

(b) Sessile liquid components following fracture

FIG. 1. Adiabatic chamber defining thermodynamic system.

2. FREE ENERGY OF THE LIQUID FILM

Consider a liquid film of uniform thickness H_C [Fig. 1(a)] resting on a horizontal surface within a closed adiabatic boundary of arbitrary shape but drawn for convenience as a cylinder with a vertical axis. The film rests upon the lower surface. The space above the film is filled with gas (air) which does not interact with the liquid. The film is taken to be on the point of breakdown and the total energy within the system is

$$\begin{aligned} E_{S1} &= (\text{Bound Energy} + \text{Free Energy}) \text{ in gas} \\ &\quad + (\text{Bound Energy} + \text{Free Energy}) \text{ in liquid} \\ &= [M_{a1}U_{a1} + (M_{a1}gH_{ga1} + A_{a1}\sigma_{SG})] \\ &\quad + [M_{l1}U_{l1} + (M_{l1}gH_{gl1} + A_C\sigma_{LG} + A_C\sigma_{LS})]. \end{aligned} \quad (1)$$

If

$$E_{FC1} = M_{l1}gH_{gl1} + A_C\sigma_{LG} + A_C\sigma_{LS} \quad (2)$$

where E_{FC1} is the free energy of the liquid film, then equation (1) can be written

$$E_{S1} = [M_{a1}U_{a1} + (M_{a1}gH_{ga1} + A_{a1}\sigma_{SG})] + M_{l1}U_{l1} + E_{FC1} \quad (3)$$

The original liquid mass is

$$M_{l1} = A_C H_C \rho$$

and if the height of its centre of gravity is

$$H_{gl1} = H_C/2$$

equation (2) can be written as

$$E_{FC1} = A_C\sigma_{LG}[1 + (\rho g H_C^2)/(2\sigma_{LG})] + A_C\sigma_{LS}. \quad (4)$$

Defining

$$He = (\rho g H_C^2)/(2\sigma_{LG}) \quad (5)$$

where He is the ratio of the potential energy of the liquid film to its surface energy in the liquid–gas interface, equation (4) becomes

$$E_{FC1} = A_C\sigma_{LG}(1 + He) + A_C\sigma_{LS} \quad (6)$$

in which the term $A_C\sigma_{LS}$ is constant for a given temperature, which fixes the magnitude of σ_{LS}, but cannot be calculated because the magnitude of σ_{LS} is unknown. A plot of equation (6) is shown in Fig. 2.

Also from equation (5)

$$H_C = [2He\sigma_{LG}/(\rho g)]^{1/2}$$

and

$$V_C = A_C[2He\sigma_{LG}/(\rho g)]^{1/2}$$

hence equation (6) may be written

$$E_{FC1} = A_C\sigma_{LG}[1 + \tfrac{1}{2}(\rho g/\sigma_{LG})(V_C/A_C)^2] + A_C\sigma_{LS}. \quad (7)$$

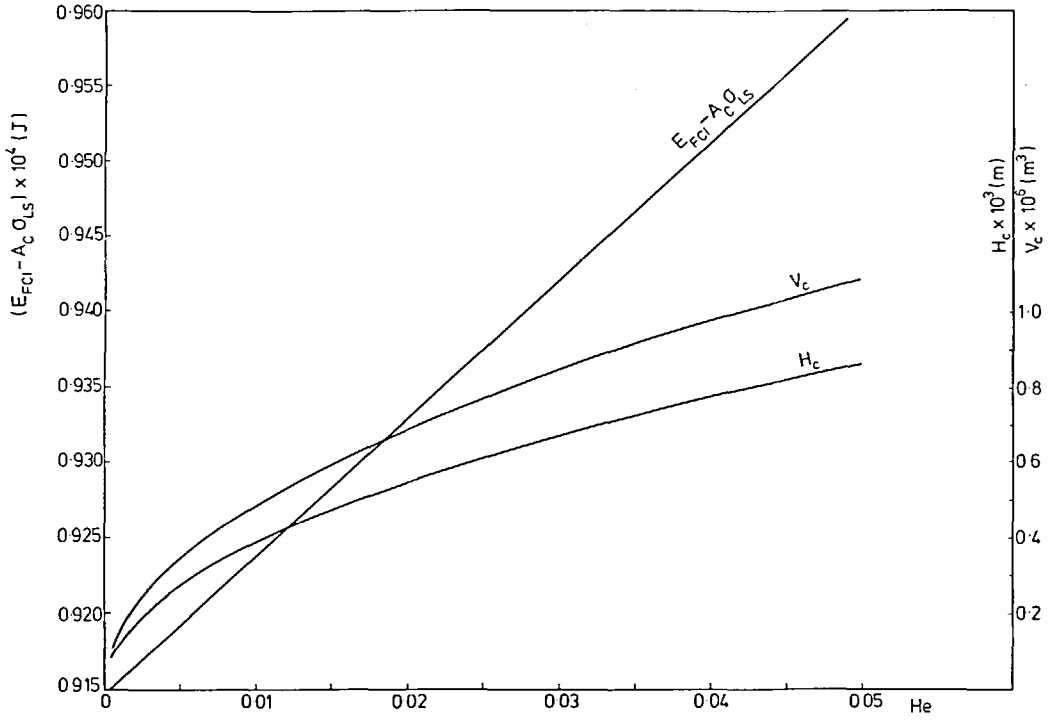

FIG. 2. Variation of free energy, thickness and volume of liquid film with *He*. $A_C = 1256.6$ mm^2 ($Ae = 168.9$).

3. FREE ENERGY OF THE LIQUID FRAGMENTS AFTER FILM BREAKDOWN

After breakdown the film will disintegrate into a number of discrete liquid fragments (or 'components') giving a situation shown conventionally in Fig. 1(b). The shape and number of the components depend upon many factors such as the texture of the surface, the nature of the liquid, the local variation in wettability, the distance the liquid is capable of moving along the surface, and so on. The total energy within the system after breakdown is the aggregate of the individual values of bound and of free energy and is given by

$$E_{S2} = [M_{a2}U_{a2}+(M_{a2}gH_{ga2}+A_{a2}\sigma_{SG})] + \left[M_{12}U_{12}+\left(\sum_1^n M_{1i}gH_{g1i}+\sum_1^n A_{21i}\sigma_{LG}\right) +\sum_1^n A_{Qli}\sigma_{LS}+\left(A_C-\sum_1^n A_{Qli}\right)\sigma_{SG}\right]. \quad (8)$$

The free energy of the components is given by

$$E_{FP} = \sum_1^n M_{1i}gH_{g1i}+\sum_1^n A_{21i}\sigma_{LG}+\sum_1^n A_{Qli}\sigma_{LS} \quad (9)$$

and

$$E_{S2} = \left[M_{a2}U_{a2}+(M_{a2}gH_{ga2}+A_{a2}\sigma_{SG}) +\left(A_C-\sum_1^n A_{Qli}\right)\sigma_{SG}\right]+M_{12}U_{12}+E_{FP}. \quad (10)$$

The formal approach followed thus far requires the recognition in both equations (1) and (8) of all the energy quantities associated with both the gas and the liquid before and after breakdown. The low density of the gas relative to the liquid renders small the potential energy change of the gas and this may be neglected. The gas-wetted area on the walls and ceiling of the system remain unchanged. To simplify understanding we assume that after breakdown a single liquid component remains resting on a reduced base. Additional gas–solid interface is therefore created and recognition of its surface energy enables us to employ Young's equation

$$\sigma_{SG}-\sigma_{LS} = \sigma_{LG}\cos\theta \quad (11)$$

where θ is the contact angle. Equation (10) now reduces to

$$E_{FP}+(A_C-A_Q)\sigma_{SG} = M_1gH_{g1}+A_2\sigma_{LG} +(A_C-A_Q)\sigma_{LG}\cos\theta+A_C\sigma_{LS}. \quad (12)$$

For the experiments to be described, it is necessary that the liquid components should have geometric or mathematical shapes permitting the calculation of M_1, H_{g1} and A_2. The most convenient bases were a circle which supported an axi-symmetric sessile drop ('drop') and an annulus which supported a toroid of symmetrical profile ('ring') (see Section 8). It was necessary to determine, for analysis, the shape of each of these profiles, which in turn permits the calculation of θ. The experimental set-up provided values for A_C and A_Q and σ_{LG} is well documented for a wide range of temperatures.

After defining the mathematical form of the profiles three functions, F_1, F_2 and F_3, can be obtained. The contact angle θ can then be obtained by solving

$$V = A_Q D F_1, \tag{13}$$

the height of the centre of gravity from

$$H_{gl} = DF_2 \tag{14}$$

and the liquid–gas interfacial area from

$$A_2 = A_Q F_3 \tag{15}$$

where F_1, F_2 and F_3 are generally functions of θ and of the dimensionless height $\bar{H} = H/D$ of the drop or ring. The dimension D is interpreted as the diameter for the drop and the radial width for the annulus.

The experimental results given later show that the profile of both the drop and the ring are quite close to the segment of a circle as shown in Fig. 3(a) provided D and θ are not large. As D and θ both increase the profile in both cases more nearly conforms to the shape shown in Fig. 3(b).

The functions F_1, F_2, F_3 are as follows. For the profile as shown in Fig. 3(a),

Drop:

$$F_1 = (2-3\cos\theta+\cos^3\theta)/(6\sin^3\theta), \tag{16}$$

$$F_2 = (1/2\sin\theta) \times \{[\tfrac{3}{4}(1+\cos\theta)^2/(2+\cos\theta)]-\cos\theta\}, \tag{17}$$

$$F_3 = 2(1-\cos\theta)/(\sin^2\theta). \tag{18}$$

Ring:

$$F_1 = (1/4\sin\theta)(\theta-\sin\theta\cos\theta), \tag{16a}$$

$$F_2 = (1/2\sin\theta) \times \{[\tfrac{4}{3}(\sin^3\theta)/(2\theta-\sin 2\theta)]-\cos\theta\}, \tag{17a}$$

$$F_3 = \theta/(\sin\theta). \tag{18a}$$

For the profile as shown in Fig. 3(b)

Drop:

$$F_1 = [1/3(1-\cos\theta)^3][4\bar{H}^3(2-3\cos\theta+\cos^3\theta)+3\bar{H}(1-\cos\theta-2\bar{H}\sin\theta)^2(1-\cos\theta) +6\bar{H}^2(1-\cos\theta-2\bar{H}\sin\theta)(\theta-\cos\theta\sin\theta)], \tag{16b}$$

$$F_2 = [\bar{H}/(1-\cos\theta)]\{1/2 - \frac{[6\bar{H}^2\sin^4\theta+3(1-\cos\theta-2\bar{H}\sin\theta)^2\sin\theta+8\bar{H}(1-\cos\theta-2\bar{H}\sin\theta)\sin^3\theta]}{[4\bar{H}^2(2-3\cos\theta+\cos^3\theta)+3(1-\cos\theta-2\bar{H}\sin\theta)^2(1-\cos\theta) +6\bar{H}(1-\cos\theta+2\bar{H}\sin\theta)(\theta-\cos\theta\sin\theta)]} - \cos\theta\}, \tag{17b}$$

$$F_3 = [1/(1-\cos\theta)^2][8\bar{H}^2(1-\cos\theta)+4\bar{H}(1-\cos\theta-2\bar{H}\sin\theta)\theta+(1-\cos\theta-2\bar{H}\sin\theta)^2]. \tag{18b}$$

Ring:

$$F_1 = [\bar{H}/(1-\cos\theta)^2][\bar{H}(\theta-2\sin\theta+\cos\theta\sin\theta+(1-\cos\theta)^2], \tag{16c}$$

$$F_2 = [\bar{H}/(1-\cos\theta)]\{\tfrac{1}{6}[4\bar{H}\sin^3\theta+3(1-\cos\theta+2\bar{H}\sin\theta)\sin^2\theta]/ [\bar{H}(\theta-\sin\theta+\cos\theta\sin\theta)+(1-\cos\theta)^2]-\cos\theta\}, \tag{17c}$$

$$F_3 = 1+\{[2\bar{H}(\theta-\sin\theta)]/(1-\cos\theta)\}. \tag{18c}$$

The definition of the profile category and the selection of the appropriate functions permit calculations of the free energy of a liquid component, whether drop or ring.

The part-elliptical profile [Fig. 3(c)] did not give a good representation for these experiments but was used successfully by one of us [6, 7] for small sessile drops axi-symmetric about a vertical axis.

4. FREE ENERGY LOSS AT FILM BREAKDOWN

Considering the system as a whole at film breakdown there can be no loss of energy, i.e. within the adiabatic boundary

$$E_{S1} = E_{S2}. \tag{19}$$

The breakdown process is, however, spontaneous and therefore irreversible and accompanied by entropy production. The expenditure of energy is necessary to modify the sizes and locations of the enclosed gas and liquid. This energy is degraded into heat by viscous action and the system temperature rises. It should in principle be possible to assess the extent of the energy degradation. In the engineering context film breakdown does not take place within an adiabatic system, but in the 'open'. This is also the case for laboratory experiments and measurements must be made in that situation. It was remarked above that gas free energy quantities are either small or unchanged and the energy dissipation or 'loss' can therefore be calculated from the change in free energy, ΔE_F, where

$$\Delta E_F = E_{FC1}-E_{FP}-(A_C-A_Q)\sigma_{SG}. \tag{20}$$

A loss coefficient may be defined as

$$\xi = \Delta E_F/(E_{FC1}-A_C\sigma_{LS}) \tag{21}$$

which, using equations (6) and (2), may be written as

$$\xi = [E_{FC1}-E_{FP}-(A_C-A_Q)\sigma_{SG}]/[A_C\sigma_{LG}(1+He)]. \tag{22}$$

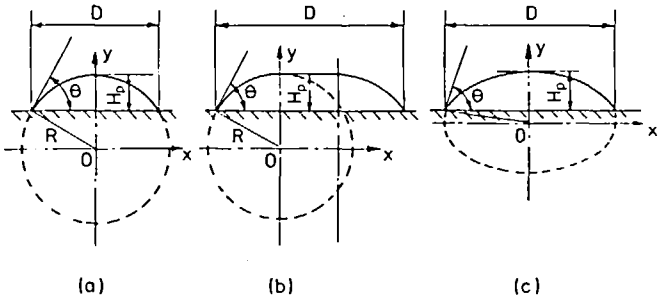

FIG. 3. Model profiles for cross section of drop or ring. (a) Circular. (b) Displaced circular. (c) Elliptical segment.

5. MINIMUM FREE ENERGY CRITERION

For a drop or a ring the first two terms on the RHS of equation (12) can be written

$$M_1 g H_{g1} = \rho g H_C^2 [F_2/(F_1 \bar{A}_Q)] A_C \qquad (23)$$

where

$$\bar{A}_Q = A_Q/A_C$$

and

$$A_2\sigma_{LG} = A_Q F_3 \sigma_{LG}. \qquad (24)$$

Substituting equations (23) and (24) into equation (12) gives

$$E_{FP} + (A_C - A_Q)\sigma_{SG} = \rho g H_C^2 [F_2/(F_1 \bar{A}_Q)] \times A_C + A_Q F_3 \sigma_{LG} + (A_C - A_Q)\sigma_{LG} \cos\theta + A_C \sigma_{LS}$$

which simplifies to

$$E_{FP} + (A_C - A_Q)\sigma_{SG} = A_C \sigma_{LG} [(2HeF_2)/(\bar{A}_Q F_1) + \bar{A}_Q F_3 + (1 - \bar{A}_Q)\cos\theta] + A_C \sigma_{LS}. \qquad (25)$$

If the liquid component has attained its steady state after breakdown its free energy should be at its minimum value. Hence $\bar{A}_Q$ corresponding to minimum free energy can be obtained by differentiating equation 25) with respect to $\bar{A}_Q$, equating to zero and solving, thus obtaining

$$(\bar{A}_Q)_{min} = \{(2HeF_2)/[F_1(F_3 - \cos\theta)]\}^{1/2}. \qquad (26)$$

Substituting equation (26) into equation (25), the minimum free energy of a stable drop or ring can be written

$$(E_{FP})_{min} + (A_C - A_Q)\sigma_{SG} = A_C \sigma_{LG} \{2[2HeF_2(F_3 - \cos\theta)/F_1]^{1/2} + \cos\theta\} + A_C \sigma_{LS}. \qquad (27)$$

In Fig. 4, the free energy expressed as

$$[(E_{FP})_{min} + (A_C - A_Q)\sigma_{SG} - A_C\sigma_{LS}],$$

calculated from equation (27), is presented together with the corresponding $(\bar{A}_Q)_{min}$ for both the drop and the ring. The free energy of the original film E_{FC1} obtained from equation (6) is also shown.

Previous investigators have assumed that the free energy of the film is conserved during breakdown and is thus equal to the aggregate free energies of the liquid components. Thus in Fig. 4 for such a case, each intersection point with the free energy curve for the film by that for a drop or a ring, gives the dimensionless number He and $(\bar{A}_Q)_{min}$ corresponding to each contact angle θ at the condition of breakdown. Figure 5 shows the variation of He and $(\bar{A}_Q)_{min}$ with θ for free energy conservation during film breakdown. Bearing in mind that

$$M_{11}U_{11} + E_{FC1} = M_{12}U_{12} + E_{FP} + (A_C - A_Q)\sigma_{SG}$$

and combining this with equations (6), (21) and (27) one may recover, after some manipulation, the relation

$$(1-\xi)^2 He^2 + 2\{(1-\xi)(1-\cos\theta - \xi) - [4F_2(F_3 - \cos\theta)/F_1]\} He + (1 - \cos\theta - \xi)^2 = 0. \qquad (28)$$

For the profile shown in Fig. 3(a), He can be obtained directly from equations (28) when θ and ξ are specified. Relations among He and $(\bar{A}_Q)_{min}$ with ξ and θ, are shown in Fig. 6. For a given ring and drop geometry it is seen from equation (28) that the loss coefficient ξ is related to the geometry of the liquid components defined by the respective values of θ and He.

For the profile shown in Fig. 3(b), equations (26) and (28) remain valid, but reference to equations (16b), (17b), (18b) for the drop and (16c), (17c) and (18c) for the ring shows that each equation now contains $\bar{H}$ thus introducing a further unknown and requiring an additional equation. These may be provided as follows:

From equation (13),

$$V = A_Q D F_1.$$

Also

$$V = A_C H_C = A_C[(2He\sigma_{LG})/(\rho g)]^{1/2}.$$

Hence

$$A_C[(2He\sigma_{LG})/(\rho g)]^{1/2} = A_Q D F_1. \qquad (29)$$

Since, for the drop

$$D = (A_C/\pi)^{1/2} 2\bar{A}_Q^{1/2}$$

and for the ring

$$D = (A_C/\pi)^{1/2}[1 - (1 - \bar{A}_Q)^{1/2}]$$

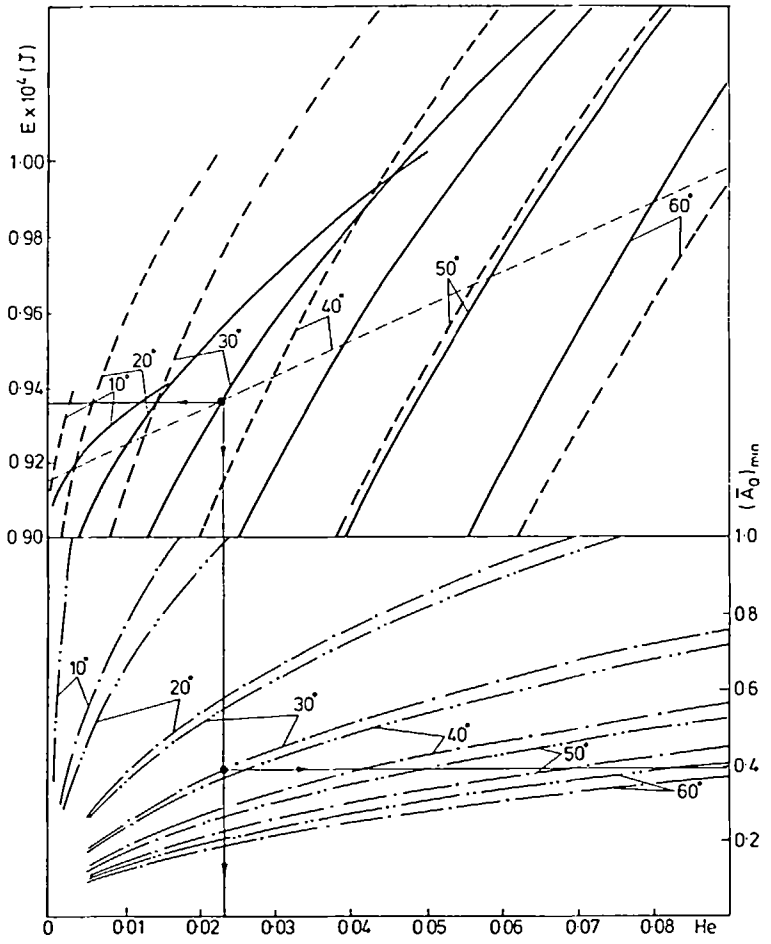

FIG. 4. Variation of free energy and area ratio for drop and ring when the profile is modelled as the segment of a circle. ——— $E = (E_{FD})_{min} + (A_C - A_Q)\sigma_{SG} - A_C\sigma_{LS}$. ———— $E = (F_{FR})_{min} + (A_C - A_Q)\sigma_{SG} - A_C\sigma_{LS}$. —·— $\bar{A}_{QD}$. —··— $\bar{A}_{QR}$. ----- Free energy of film, $E = E_{FC} - A_C\sigma_{LS}$.

then substituting D into equation (29) and defining

$$Ae = \rho g A_C/\sigma_{LG} \tag{30}$$

which is directly proportional to the cube of the ratio of the diameter of unbroken film to its thickness (D_C/H_C), one obtains for the drop

$$He = (2/\pi)Ae\bar{A}_{QD}^3 F_1^2 \tag{31}$$

and for the ring

$$He = [Ae\bar{A}_{QR}^2/(2\pi)][1-(1-\bar{A}_{QR}^2)^{1/2}F_1^2]. \tag{32}$$

Equations (31) and (32) are the additional equations required for relating He, ξ, $(\bar{A}_Q)_{min}$ and $\bar{H}$ for the profile shown in Fig. 3(b).

6. EXPERIMENTAL METHOD

The apparatus is shown in Fig. 7(a) and the test block with the prepared surface in Fig. 7(b). The surface treatment is described below.

The test block with the surface fully prepared rests on an adjustable surface carefully levelled to the horizontal. A liquid film is formed, using a water syringe, to cover the entire area within the diameter D_E [Fig. 7(b)]. The film is then made progressively thinner by the slow withdrawal of liquid and its diminishing thickness is closely monitored by the micrometer microscope (magnification factor 35) in order to obtain the thickness at breakdown. Immediately after breakdown the respective maximum heights of the drop and of the ring are measured. Liquid weights are forthwith determined with a high precision balance by weighing the wet block, then removing one liquid component with absorbent tissue and reweighing. The weight of the dry block is known. To ensure no significant evaporation of drop or ring occurred during measurements, observations were made of the time rates of evaporation. Evaporation during measurements was found to be negligible.

It was not feasible to determine drop and ring contact angles using a goniometer. Reasonably satisfactory results were obtained by photography in the plane of the prepared surface, the camera and lighting being arranged to show the required angle in silhouette

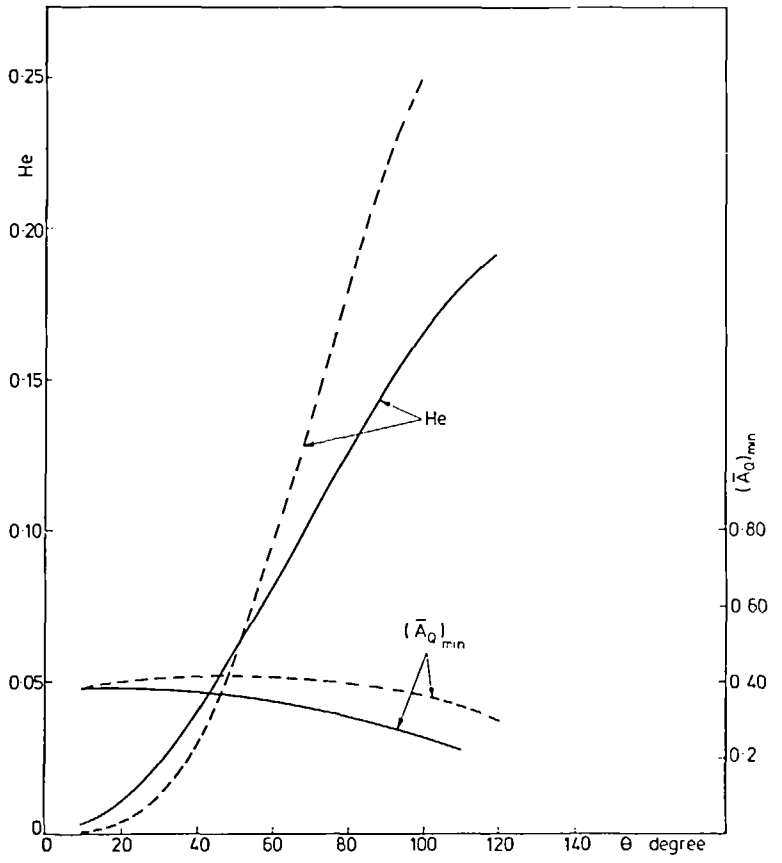

FIG. 5. Variation of He and $(\bar{A}_Q)_{min}$ with θ when the profile is the segment of a circle. ——— Drop. – – – Ring.

enabling the direct measurement of the angle between the base and the tangent to the triple point. To photograph drop contact angles it was necessary first to remove the ring.

7. PREPARATION OF THE TEST SURFACE

To perform this experiment successfully the following capillary conditions must be met concurrently by the test surface at the instant of film breakdown:

(a) All liquid must migrate to the wettable surfaces.
(b) The wettable surfaces must be completely covered by liquid.
(c) The geometry of the liquid components must permit the calculation of liquid–gas surface area and of the location of the centre of gravity.

We spent many weeks attempting to fulfil these deceptively simple conditions. Block materials tried were glass, steel and PTFE. Glass was the final choice. The working surface was ground with silicon carbide powder of average grain size 9 μm and size range 3–19 μm to obtain a fine matt surface. The surface was then masked with adhesive paper exposing only the surfaces which were to be non-wetting. These surfaces were treated with PTFE spray. The masking paper was finally removed after the non-wettable surfaces had been gently polished with paper tissue.

About 30 combinations of block material, geometric shapes and dispositions and surface treatment were tried with limited success. Typical problems were ruptures in migrating liquid which left residues on the non-wetting area suggesting a limit to the distance water would travel while remaining intact; also the excessive provision of wettable area which was only partially filled.

Two successful test blocks A and B were studied. Their respective dimensions are given in Fig. 7(b). There may be other geometries and methods of preparation which are also adequate.

8. CONCLUSIONS

This work leads to the following conclusions for a horizontal surface:

(1) It is possible to determine experimentally the loss of aggregate free energy which accompanies the

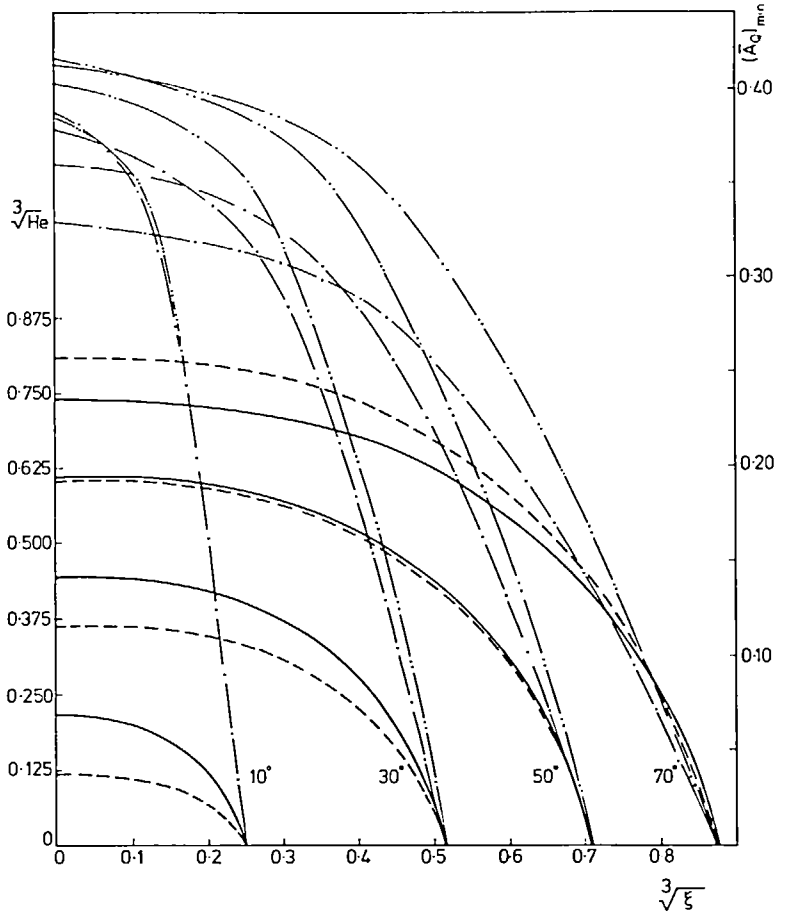

FIG. 6. Relations among *He*, ξ and $(\bar{A}_Q)_{min}$. ——— *He* for drop. ----- *He* for ring. —·— $(\bar{A}_{QD})_{min}$. —··— $(\bar{A}_{QR})_{min}$.

breakdown of a stationary liquid film. To accomplish this it is necessary to employ a simple geometry for the test surface; in this case a circular area surrounded at some distance by a narrow annular area both rendered wettable. The wider intervening annular area was made non-wetting.

(2) The liquid film wetting an annulus has a cross section which can be modelled by a circular segment [Fig. 3(a)] for small contact angle and a small width. For a larger width the section is a narrow plane between ends which are circular arcs [Fig. 3(b)]. The model shown in Fig. 3(a) was generally used throughout this work.

(3) The conditions in conclusion (2) apply also to the

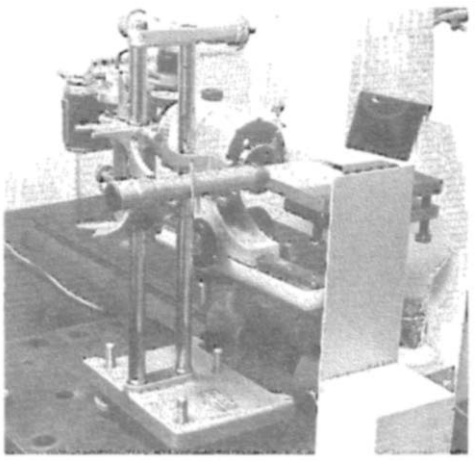

FIG. 7(a). General view of apparatus.

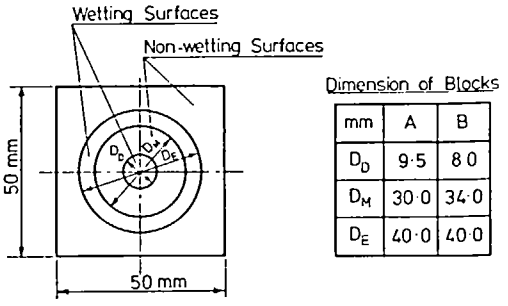

Dimension of Blocks

mm	A	B
D_D	9·5	8·0
D_M	30·0	34·0
D_E	40·0	40·0

FIG. 7(b). Test block (thickness 9.2 mm).

Table 1. Comparison of the contact angle of the drops, D_D = 8.0 mm

Type of drop	Height H (mm)	Weight W (mg)	Contact angle Profiles a	b (degree)	c	Experimental value (degree)
	2.746	114.0	84.7	101.5	151.6	98.0
	2.110	81.0	70.6	86.6	121.9	81.0
	1.676	63.0	60.3	77.8	125.5	60.0
(a)	1.301	50.0	51.1	72.4	137.6	51.0
	0.983	39.0	41.6	65.6	148.9	40.0
	0.809	32.0	35.0	57.6	153.1	33.0
	0.576	27.0	30.2	93.0	170.2	30.0
	0.376	21.0	23.8	—	—	24.0
	0.231	17.0	19.6	—	—	18.0
	0.694	21.0	23.8	27.2	47.3	25.0
	0.723	22.0	24.9	28.5	50.3	24.0
	0.636	22.5	25.5	35.1	132.9	24.0
	0.723	22.5	25.5	29.7	59.1	24.0
(b)	0.665	18.0	20.6	21.5	25.3	18.0
	0.549	13.0	15.0	15.9	15.9	15.0
	0.607	15.0	17.2	17.5	17.5	17.0
	0.549	13.0	15.0	15.9	15.8	16.0

(a) Liquid placed for measurement purposes, i.e. no prior film breakdown.
(b) Following film breakdown.

sessile drop. For a large contact angle and small diameter, the segment of an ellipse [Fig. 3(c)] gives a closer model.

(4) Tables 1 and 2 show that the experimental measurements of contact angle θ show good agreement for both ring and drop if these are considered to have the profile shown in Fig. 3(a). Profiles in Figs. 3(b) and 3(c) clearly provide less satisfactory models. For the case of the profile shown in Fig. 3(a), Fig. 9 gives a comparison of the calculated and measured values. The agreement is generally close for the drops. For the ring the agreement is good at low values of θ but worsens progressively with increasing values of θ. This occurs because the ring profile is not quite symmetrical about its centre causing an increase in θ on the inside and a decrease in θ on the outside. The asymmetry arises from an inward component of surface tension. It is not possible to employ silhouette photography to determine θ on the inside of the ring, but it is reasonable to suppose that its value would be greater than that calculated and present an error trend similar to that shown on Fig. 9 and defining a mean between inside and outside values in general agreement with calculated values.

(5) The curves of energy loss coefficient ζ shown in Fig. 8 suggest that the losses increase both with the increase in non-wetting area to be crossed by the migrating liquid and also with the increase in He; the

Table 2. Comparison of the contact angle of the rings, D_E = 40.0 mm, D_M = 34.0 mm

Type of ring	Height H (mm)	Weight W (mg)	Contact angle Profile a	b (degree)	c	Experimental values (degree)
	1.214	355.0	83.5	92.4	108.1	67.0
	0.954	309.0	76.9	105.2	139.8	57.0
	0.694	241.0	65.3	121.8	158.1	49.0
(a)	0.520	153.0	46.0	64.5	129.8	41.0
	0.405	116.0	36.0	50.1	124.1	30.0
	0.289	83.0	26.6	38.6	134.6	22.0
	0.173	64.0	20.6	20.2	175.7	19.0
	0.462	120.0	37.2	41.6	59.6	34.0
	0.491	134.0	41.1	49.6	88.3	34.0
	0.636	170.0	50.2	56.7	79.4	40.0
(b)	0.809	200.0	57.1	57.5	58.6	48.0
	0.462	113.0	35.3	36.5	40.4	30.0
	0.549	134.0	41.1	42.1	44.9	41.0

(a) Liquid placed for measurement purposes, i.e. no prior film breakdown.
(b) Following film breakdown.

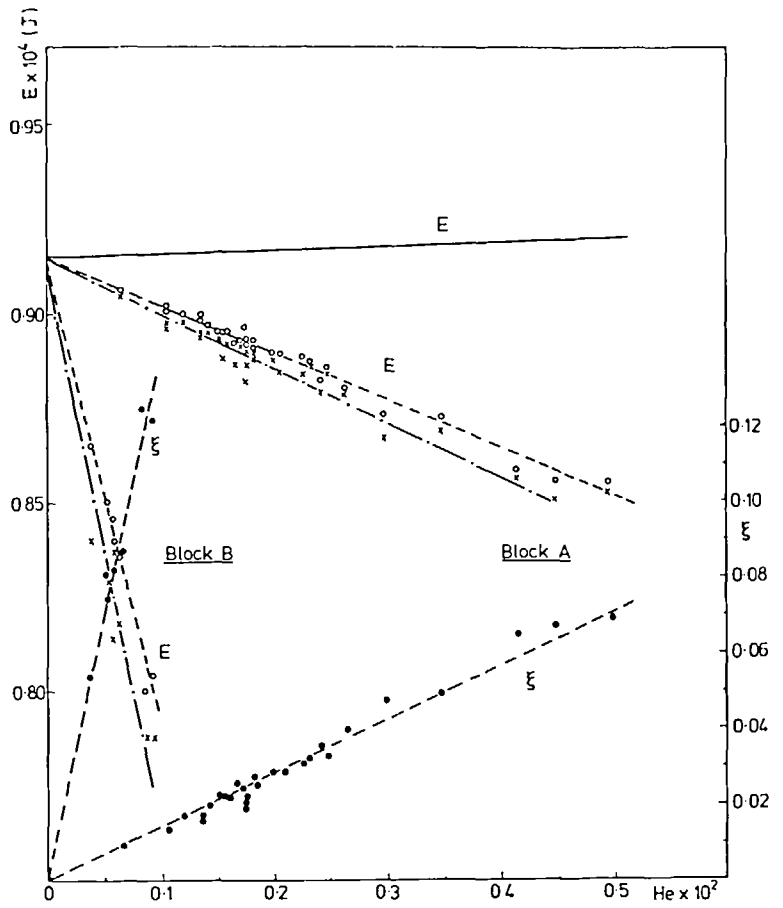

FIG. 8. Free energy loss at film breakdown ——— $E = E_{FC1} - A_C\sigma_{LS}$. Profile, Fig. 3(a): —○— $E = (E_{FP})_{min} + (A_C - A_Q)\sigma_{SG} - A_C\sigma_{LS}$. —●— ξ. Profile, Fig. 3(b): ——— $E = (E_{FP})_{min} + (A_C - A_Q)\sigma_{SG} - A_C\sigma_{LS}$.

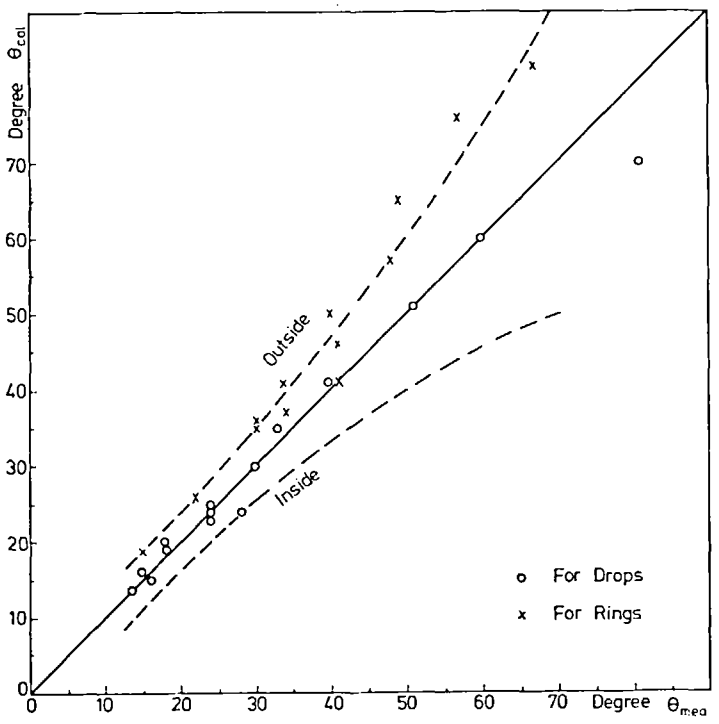

FIG. 9. Comparison of the contact angles obtained from measurement and from calculation when the profile is modelled by a circular segment.

ratio: potential energy/surface energy. The former suggests fluid friction losses in transit; the reason for the latter is not clear. Especially interesting is the linear variation of ξ with He for both cases A and B.

(6) Qualitative observations from many unsuccessful attempts show that migrating liquid is liable to rupture in transit across a non-wetting area and is restricted in the distance it can travel. Liquid fragments may come to rest on a non-wetting surface and will not necessarily spread to cover a wettable surface. It might have been useful to have taken high speed magnified photographs of the act of film breakdown.

(7) It is to be expected that conclusions (5) and (6) will apply with some modification to flowing films on horizontal surfaces and to a limited extent on inclined plane surfaces.

Work is continuing in our Laboratory and we are currently studying a moving film propelled by steam drag along an instrumented flat plate located within our wet steam tunnel.

Acknowledgements—The experimental work was carried out in the Wet Steam Laboratory, University of Liverpool, in 1981–1982. We are grateful to Mr. Eric Hughes who helped with the construction of apparatus and the experimental work.

REFERENCES

1. D. E. Hartley and W. Murgatroyd, Criteria for the break-up of thin liquid layers flowing isothermally over a solid surface, *Int. J. Heat Mass Transfer* **7**, 1003–1015 (1964).
2. W. Murgatroyd, The role of shear and form forces in the stability of a dry patch in two-phase film flow, *Int. J. Heat Mass Transfer* **8**, 297–301 (1965).
3. S. G. Bankoff, Minimum thickness of a draining liquid film, *Int. J. Heat Mass Transfer* **14**, 2143–2146 (1971).
4. J. Mikielewicz and J. R. Moszynski, Minimum thickness of a liquid film flowing vertically down a solid surface, *Int. J. Heat Mass Transfer* **19**, 771–776 (1976).
5. B. H. Khoshaim, The flow of rivulets over L.P. steam turbine guide blades, Ph.D. Thesis, The University of Liverpool (1975).
6. D. J. Ryley and B. H. Khoshaim, A new method of determining the contact angle made by a sessile drop upon a horizontal surface. *J. Coll. Interface Sci.* **59**, 243–251 (1977).
7. D. J. Ryley and M. S. B. Ismail, The shape of sessile water drops on inclined plane surface, *J. Coll. Interface Sci.* **65**, 394–396 (1978).

PERTE D'ENERGIE LIBRE DURANT LA RUPTURE DES FILMS LIQUIDES

Résumé—La surface plane d'un bloc de verre horizontal est traitée de façon que quelques aires sont mouillées par l'eau et d'autres sont répulsifs vis-à-vis de l'eau. Une aire circulaire (mouillable, "goutte") est entourée par un anneau (non mouillable) lui-même entouré par un second anneau étroit (mouillable "anneau"), tous les cercles étant concentriques.

Un film liquide est formé sur l'aire entière dans le cercle extérieur. Il est diminué en épaisseur jusqu'à ce que la perforation se produit et l'eau résiduelle se rassemble et couvre chaque aire mouillable. Des mesures de hauteur et de masse liquide sont faites à la fois pour les films original et final, pour la goutte et l'anneau. Ces mesures permettent le calcul de l'energie libre et les énergies finales des aggrégats.

Il apparait une chute d'énergie qui peut être reliée à la masse du film et à la géométrie des surfaces et elle peut être calculée en modélisant les profils de l'anneau et de la goutte par des formes qui permettent l'analyse. Un segment circulaire donne le meilleur essai.

Des angles de contact calculés à partir des modèles sont vérifiés par des mesures sur les photographies.

Deux nouveaux nombres sans dimension sont introduits dans l'analyse; $He = \rho g H_c^2/2\sigma_{LG}$ qui est le rapport énergie potentielle/énergie capillaire pour un composant liquide, et $Ae = \rho g A_c/\sigma_{LG}$ qui est relié au rapport diamètre original de la surface solide mouillee/epaisseur du film.

DIE VERLUSTE AN FREIER ENERGIE WÄHREND DES AUFREISSENS VON FLÜSSIGKEITSFILMEN

Zusammenfassung- Diese Untersuchung wurde im Zusammenhang mit einer laufenden Untersuchung des Aufreißverhaltens von Flüssigkeitsfilmen an den Leitschaufeln von Naßdampfturbinen durchgeführt. Die ebene Oberfläche eines horizontalen Glasblocks wurde so behandelt, daß einige Flächenteile mit Wasser benetzbar, andere wasserabweisend waren. Eine runde Fläche (benetzbar, "Tropfen") war von einem ringförmigen Streifen (nicht benetzend) umgeben, der wiederum von einem engen zweiten ringförmigen Streifen (benetzbar, "Ring") umgeben war, wobei alle Kreise konzentrisch waren.

Ein Flüssigkeitsfilm wird auf die gesamte Fläche innerhalb des äußeren Kreises aufgebracht. Dessen Dicke wird vermindert, bis sich Löcher bilden und das restliche Wasser sich auf den benetzbaren Flächen sammelt und diese bedeckt. Messungen der Filmhöhe und der Flüssigkeitsmasse wurden sowohl für den ursprünglichen Film als auch später für den Tropfen und den Ring durchgeführt. Diese Messungen ermöglichen die Berechnung sowohl der ursprünglichen Freien Energie als auch der gesamten restlichen Freien Energien. Es tritt ein Energieverlust auf, der mit der Masse des Films und der Geometrie der behandelten Oberflächen in Verbindung gebracht und berechnet werden kann, wenn die Profile auf Ring und Tropfen durch geometrische Formen beschrieben werden können, die eine Berechnung zulassen. Die Beschreibung durch ein Kreissegment erwies sich als am besten. Die Kontaktwinkel, die aus den beschriebenen Profilen berechnet wurden, wurden durch Messungen an Fotografien der Umrisse überprüft. Zwei neue dimensionslose Kennzahlen wurden in die Berechnung eingeführt: $He = \rho g H_c^2/2\sigma_{LG}$, das Verhältnis der potentiellen Energie zur Oberflächenenergie für eine flüssige Komponente und $Ae = \rho g A_c/\sigma_{LG}$, eine Größe, die mit dem Verhältnis des Durchmessers der festen Oberfläche, die vom Originalfilm benetzt wurde, zur Filmdicke in Zusammenhang steht.

ПОТЕРИ СВОБОДНОЙ ЭНЕРГИИ ПРИ ОТРЫВЕ ПЛЕНОК ЖИДКОСТИ

Аннотация — Настоящее исследование было начато как дополнение к проводимому изучению поведения отрывных пленок жидкости, пересекающих лопасти статора турбин, работающих на влажном паре.

Плоская поверхность горизонтального стеклянного блока обрабатывалась таким образом, чтобы некоторые ее области смачивались водой, а другие оказались водоотталкивающими. Круг (смачиваемая область, "капля") находится внутри кольца (несмачивающего), которое, в свою очередь, окружено вторым узким кольцом (смачиваемым, "кольцо"), причем все окружности концентрические.

Пленка жидкости образуется над всей областью внутри внешнего круга. Толщина этой пленки уменьшается то тех пор, пока не наступает перфорация, остатки воды накапливаются и покрывают каждую из смачиваемых областей. Измерения высоты и массы жидкости проведены как для первоначальной пленки, так и в последующем для капли и кольца. Данные этих измерений позволяют рассчитать как исходную, так и конечную свободную энергию.

Происходит потеря энергии, которую можно связать с массой пленки и геометрией поверхностей и рассчитать профили кольца и капли с помощью соответствующих моделей. Лучшие результаты получены с помощью модели кольцевого сегмента.

Контактные углы, рассчитанные по модельным профилям, сравнивались с экспериментальными на фотографиях.

Были использованы два новых безразмерных числа: $He = \rho g H_C^2/2\sigma_{LG}$ отношение потенциальной энергии к поверхностной для жидкой компоненты, и $Ae = \rho g A_C/\sigma_{LG}$ — отношение диаметра смачиваемой поверхности к толщине пленки.